European Radiology (2019) 29:5528–5538
https://doi.org/10.1007/s00330-019-06069-z

NEURO

A radiomics nomogram based on multiparametric MRI might stratify glioblastoma patients according to survival

Xi Zhang[1] · Hongbing Lu[1] · Qiang Tian[2] · Na Feng[3] · Lulu Yin[1] · Xiaopan Xu[1] · Peng Du[1] · Yang Liu[1]

Received: 1 August 2018 / Revised: 6 January 2019 / Accepted: 4 February 2019 / Published online: 7 March 2019

Abstract

Objectives To construct a radiomics nomogram for the individualized estimation of the survival stratification in glioblastoma (GBM) patients using the multiregional information extracted from multiparametric MRI, which could facilitate the clinical decision-making for GBM patients.

Materials and methods A total of 105 eligible GBM patients (57 in the long-term and 48 in the short-term survival groups, separated by an overall survival of 12 months) were selected from the Cancer Genome Atlas. These patients were divided into a training set ($n = 70$) and a validation set ($n = 35$). Radiomics features ($n = 4000$) were extracted from multiple regions of the GBM using multiparametric MRI. Then, a radiomics signature was constructed using least absolute shrinkage and selection operator regression for each patient in the training set. Combined with clinical risk factors, a radiomics nomogram was constructed based on a multivariate logistic regression model. The performance of this radiomics nomogram was assessed by calibration, discrimination, and clinical usefulness.

Results The radiomics signature consisted of 25 selected features and performed better than clinical risk factors (i.e., age, Karnofsky performance status, and treatment strategy) in survival stratification. When the radiomics signature and clinical risk factors were combined, the radiomics nomogram exhibited promising discrimination in the training (C-index, 0.971) and validation (C-index, 0.974) sets. The favorable calibration and decision curve analysis indicated the clinical usefulness of the radiomics nomogram.

Conclusions The presented radiomics nomogram, as a non-invasive prediction tool, could exhibit a favorable predictive accuracy and provide individualized probabilities of survival stratification for GBM patients.

Key Points

- *Non-invasive survival stratification of GBM patients can be obtained with a radiomics nomogram.*
- *The proposed nomogram constructed by radiomics signature selected from 4000 radiomics features, combined with independent clinical risk factors such as age, Karnofsky performance status, and treatment strategy.*
- *The proposed radiomics nomogram exhibited good calibration and discrimination for survival stratification of GBM patients in both training (C-index, 0.971) and validation (C-index, 0.974) sets.*

Keywords Multiparametric MRI · Glioblastoma · Machine learning · Nomogram

Xi Zhang and Hongbing Lu contributed equally to this work.

Electronic supplementary material The online version of this article (https://doi.org/10.1007/s00330-019-06069-z) contains supplementary material, which is available to authorized users.

✉ Yang Liu
yliu@fmmu.edu.cn

[1] School of Biomedical Engineering, Fourth Military Medical University, No.169, Changle West Road, Xi'an 710032, Shaanxi, People's Republic of China

[2] Department of Radiology, Tangdu Hospital, Fourth Military Medical University, 569 Xinsi Road, Xi'an 710038, Shaanxi, People's Republic of China

[3] Department of Physiology (N.F.), Fourth Military Medical University, 169 Changle West Road, Xi'an 710032, Shaanxi, People's Republic of China

Abbreviations

2D	Two-dimensional
3D	Three-dimensional
AUC	Area under the curve
DCA	Decision curve analysis
FLAIR	Fluid-attenuated inversion recovery
GBM	Glioblastoma
IDH	Isocitrate dehydrogenase
KPS	Karnofsky performance status
LASSO	Least absolute shrinkage and selection operator
MGMT	Methylated O^6-methylguanine-DNA methyltransferase
OS	Overall survival
rCET	The region of contrast-enhanced tumor
rE/nCET	The region of edema/non-contrast-enhanced tumor
rEA	The region of entire abnormality
rNec	The region of necrosis
TCGA	The Cancer Genome Atlas
TCIA	The Cancer Imaging Archive
TE	Echo time
TR	Repetition time

Introduction

Glioblastoma (GBM) is the most common malignant primary brain tumor [1]. Despite advances in surgery plus chemoradiotherapy, the median survival of GBM patients remains 10–14 months [2]. A minority of GBM patients can survive longer than 36 months [3, 4]. The stratification of prognosis groups is greatly needed toward a more reasonable and personalized approach [5] and will directly influence GBM evaluations, targeted treatments, and follow-up management [6].

In current clinical practice, several prognostic factors are commonly used to predict the prognoses of GBM patients, including age, gender, Karnofsky performance status (KPS) [7], the presence of a unilateral or bilateral tumor [8], and molecular profiling [9]. However, the spatial and temporal pathological heterogeneity of GBM limits the ability of these indices to fully capture GBM characteristics [10]. As a non-invasive and preoperative routine examination for GBM [11], the magnetic resonance imaging (MRI) can provide a comprehensive and macroscopic image of the entire tumor [12]. Currently, MRI techniques have demonstrated great potential in the prediction of the survival of GBM patients [13–15]; however, the ability to discriminate between long- and short-term survival groups must be improved.

In common MRI acquisitions, four image sequences, i.e., T1-weighted gadolinium contrast-enhanced (T1C), T1-weighted (T1), T2-weighted (T2), and T2-weighted fluid-attenuated inversion recovery (FLAIR) sequences, are recommended for the diagnosis of a brain tumor [11]. It is widely believed that multiparametric MRI can improve the diagnostic efficiency and performance of survival stratification [16]. Moreover, as seen on MRI, GBM varies across geographical regions, including enhanced, necrotic, and non-enhanced regions, which all contribute to prognosis prediction [14, 15, 17]. More recently, radiomics has been introduced to map MRI images to quantitative data and extend the clinical and genomic information to generate radiomics signatures to improve clinical decision-making, e.g., diagnostic, prognostic, and therapeutic evaluations [18, 19]. A multiparametric MRI- and multiregion-based radiomics approach may improve the performance of the survival stratification in GBM patients.

As a graphical depiction of a predictive statistical model, a nomogram can incorporate several factors and provide an individualized estimation of patient outcomes [20–25]. Thus, a radiomics nomogram, which combines radiomics signature and clinical information, may be an easy-to-use and more accurate tool for physicians to stratify GBM patients.

The purpose of this study was to develop and validate a multiparametric MRI- and multiregion-based radiomics nomogram for the individualized estimation of the survival stratification in GBM patients.

Materials and methods

Patient population and study design

According to the inclusion criteria presented (Fig. 1), a total of 262 patients (i) with clinical information (such as overall survival of patients) from the Cancer Genome Atlas (TCGA) [26] GBM Project and (ii) the corresponding MRI data from the Cancer Imaging Archive (TCIA) [27] were retrospectively included. Then, 157 patients were excluded for the reasons listed below: (i) lack of at least one of the following MRI sequences from TCIA: T1-weighted gadolinium contrast-enhanced, T1-weighted, T2-weighted, and T2-weighted FLAIR sequences (T1C, T1, T2, FLAIR) ($n = 107$); (ii) the MRI sequences were acquired after surgery or biopsy ($n = 33$); (iii) the MRI sequences were acquired with severe motion or artifacts that may have induced bias in subsequent analyses ($n = 17$). After that, a total of 105 GBM patients were retrospectively included in our study. All the patients were separated into two groups according to overall survival (OS); i.e., 57 patients were included in the long-term survival group (OS ≥ 12 months) and 48 patients were included in the short-term survival group (OS < 12 months). Next, the patients were randomly separated into a training cohort ($n = 70$) and a validation cohort ($n = 35$) at a ratio of 2:1. In this retrospective study, the requirement for informed consent was waived because all the patient data in TCGA was deidentified.

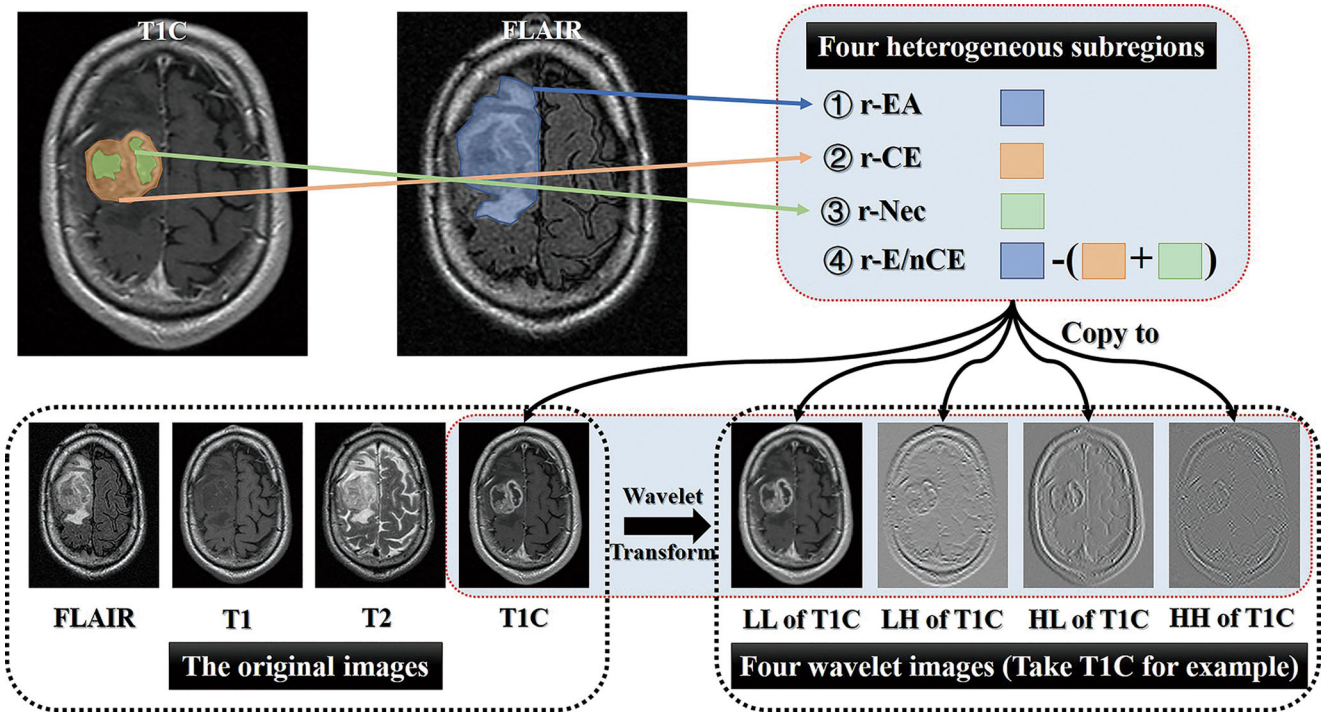

Fig. 1 The generation of four heterogeneous regions in the images of glioblastoma patient and the wavelet transform process for each MRI sequence. Using the T1C image data, for example, the original T1C image was decomposed into four new images in four decomposed directions (LL, LH, HL, and HH) by wavelet transform. L and H represent low-pass and high-pass functions, respectively

In addition to the multiparametric MRI data, the clinical data for all patients, including age, gender, KPS, isocitrate dehydrogenase (IDH) status, and intervention method, were also obtained from support documents of the TCGA GBM Project. Moreover, via review of the multiparametric MRI data, the tumor location information of each patient was acquired for further analysis.

Imaging data acquisition and preprocessing

All 105 patients underwent four MRI modalities, i.e., T1C, T1, T2, and FLAIR sequence. The T1C sequence was acquired with the following range of parameters: repetition time (TR)/echo time (TE), 4.9–3285 msec/2.1–20 msec; slice thickness, 1–5 mm; spacing slice, 0.6–7.5 mm. The T1 sequence was acquired with the following range of parameters: TR/TE, 352–3379 msec/2.75–19 msec; slice thickness, 1–5 mm; spacing slice, 2–7.5 mm. The T2 sequence was acquired with the following range of parameters: TR/TE, 700–6370 msec/15–120 msec; slice thickness, 1.5–5 mm; spacing slice, 1.5–7.5 mm. The FLAIR sequence was acquired with the following range of parameters: TR/TE, 6000–11,000 msec/34.6–155 msec; slice thickness, 2.5–5 mm; spacing slice, 2–7.5 mm. The matrix size of all the MRI sequences was either 256 × 256 or 512 × 512.

Diverse parameters of different MRI sequences were used during image acquisition, which may have a great influence on three-dimensional (3D) analyses; thus, two-dimensional (2D) preprocessing was performed in this study. First, image registration was performed to register the T1, T2, and FLAIR sequence images to the T1C sequence images for each patient. Next, the planar resolution of each modality was uniformly resampled to 256 × 256. Finally, the image contrast of each modality was normalized using the Collewet normalization algorithm (mean ± 3 sigma) to correct for the effects of different acquisition protocols and magnetic field strengths [28]. However, bias field correction methods were not applied to correct for intensity non-uniformities caused by the inhomogeneity of the scanner's magnetic field during image acquisition. The reason is that, in preliminary experiment, we observed that application of such algorithm would obliterate the T2-FLAIR signal. All the processing was performed using a custom-developed package using MATLAB 2015b (MathWorks).

Multiregional delineation

As illustrated in Fig. 1, the following four heterogeneous regions were manually drawn: (1) entire abnormality (rEA) on FLAIR image, (2) contrast-enhanced tumor (rCET) and (3) necrosis (rNec) on T1C image, in addition, (4) the region of edema/non-contrast-enhanced tumor (rE/nCET) as defined by rEA–rCET–rNec. Then, these four regional contours were respectively mapped to each MRI sequence for each patient

based on spatial transformations from the registration. In this study, all the manual contours were created by two neuroradiologists with 12 and 8 years of MRI interpretation experience. They blinded to the clinical information about patients and worked together on outlined contours of each patient for consensus reading, especially on those with discrepancy. Furthermore, we performed the multiregional segmentation on the slice which (1) include all the four types of regions, and (2) contain the largest tumor area for each patient. Based on this selection criterion, the information of each heterogenous region could be extracted and analyzed.

OS status-related radiomics feature extraction and radiomics signature construction

To extract high-throughput features, both the original image in each MRI sequence and four corresponding wavelet-filtered images were obtained (Fig. 1). A total of 4000 radiomics features were finally extracted for each subject. A detailed description of the feature extraction is provided in Appendix E1, section S2 (online).

To reduce the radiomics feature dimensions and identify the features that were highly effective for describing the prognosis of GBM patients, the least absolute shrinkage and selection operator (LASSO) regression algorithm [29] was adopted to select the OS status-related features among the 4000 radiomics features in the training cohort. Regulated by λ, the LASSO method can shrink all the coefficients toward zero and sets the coefficients to zero for irrelevant features. Then, 10-fold cross-validation with a maximum area under the curve (AUC) criterion was employed to find an optimal λ, in which the final value of λ yielded the maximum AUC. The features with non-zero coefficients were used to construct the regression model, and the corresponding non-zero coefficients were defined as the Rad-score. The fitting formula was generated using a linear combination of the values of the selected features that were weighted by their Rad-score. The formula was then used to calculate a radiomics signature for each GBM patient to reflect their long- or short-term OS.

Construction and assessment of the radiomics nomogram with the training cohort

The radiomics signature and each clinical factor were first inserted into a univariate logistic regression model to test whether they were significantly independent prognostic factors for OS stratification in the training cohort. The radiomics signature and significant clinical factors were then utilized to build the multivariate logistic regression model to discriminate the short- and long-term OSs of the GBM patients. For comparison, multivariate logistic regression models that used only the significant clinical factors or the radiomics signature were also established. Finally, a radiomics nomogram, which could visually and individually indicate the probability of OS stratification in the training cohort, was constructed based on multivariate logistic regression [30].

The discriminative ability of the radiomics nomogram was quantitatively measured using the C-index, which ranges from 0 to 1. The Hosmer-Lemeshow test was performed to evaluate the goodness-of-fit of the radiomics nomogram. The calibration curves were plotted using observed probabilities and the nomogram-estimated probabilities [30, 31].

External validation of the radiomics nomogram on the validation cohort

The fitting formula that was constructed with the training cohort was applied to all GBM patients in the validation cohort, and the radiomics signature of each patient was calculated. The radiomics nomogram was then validated in this cohort using the radiomics signatures and clinical factors. Finally, the C-index and the Hosmer-Lemeshow test were implemented to evaluate the model results for OS stratification. Moreover, the calibration curve was also constructed.

Clinical utility of the radiomics nomogram

To estimate the clinical utility of the radiomics nomogram, decision curve analysis (DCA) was performed by calculating the net benefits at different threshold probabilities in the combined training and validation cohorts [32].

Statistical analysis

In this study, either Student's *t* tests or Mann-Whitney *U* tests were applied to confirm whether inter-group differences in continuous variables (such as age) existed between the short- and long-term OS groups. Either chi-square tests or Fisher's exact tests were performed on the rest of the categorical characteristics to determine whether the constituent ratios were significantly different between the groups. All statistical analyses were performed with R software version 3.4.2. (R Foundation for Statistical Computing; http://www.R-project.org, 2017), using basic statistical functions or additional packages. The following R packages were used: the *glmnet* package was used for the LASSO logistic regression, the *rms* package was used for the nomograms and calibration curves, the *Hmisc* package was used for the comparisons between the C-indices, the *Resource Selection* package was used to apply the Hosmer-Lemeshow tests, and the *rmda* package was used to implement the DCA.

Results

Clinical characteristics of the patients

The clinical characteristics and corresponding results of the statistical analyses comparing the long- and short-term OS groups are summarized in Table 1. The two groups significantly differed in age and KPS in both the training and validation cohorts.

Radiomics signature construction

To determine the optimal regulation weight λ ($\lambda = 0.07998$, $\log(\lambda) = -2.52592$) for the LASSO algorithm, 25 features with non-zero coefficients were selected for survival stratification among the 4000 radiomics features (Fig. 2). The details of these 25 features are described in Appendix E1, section S3 (online). Then, the radiomics signature was constructed by the fitting formula listed in Appendix E1, section S4 (online), in which the 25 selected features were ordered by the absolute values of their coefficients. The radiomics signatures for each GBM patient in the training and validation cohorts are presented in Fig. 3. The patients with long-term OS generally displayed a significantly higher radiomics signature than the patients with short-term OS in both the training ($p < 0.001$) and validation ($p < 0.001$) cohorts (Table 1).

Non-zero-coefficient features analysis

As mentioned above, 25 radiomics features with non-zero coefficient were selected by LASSO algorithm and ordered by their absolute values of coefficients which were seen in the calculating formula of radiomics signature in Appendix E1, section S4 (online). The absolute value of coefficient can be seen as the importance of certain feature to the OS stratification. For different heterogenous regions, the sum of absolute coefficients of features from rEA was 1.597, higher than the sum of feature coefficients from other regions, according to Table 2. For different MRI sequences, the sum of absolute coefficients of features from FLAIR was 1.631, higher than the sum of other sequences. Combining both the

Table 1 Characteristics of patients in the training and validation cohorts

	Training cohort ($n = 70$)			Validation cohort ($n = 35$)		
	Short-term ($n = 32$)	Long-term ($n = 38$)	p	Short-term ($n = 16$)	Long-term ($n = 19$)	p
Age, mean ± SD	62.91 ± 10.14	54.6 ± 16.04	*0.011*	63.50 ± 12.11	54.05 ± 11.02	*0.021*
Gender, no. (%)			0.695			0.072
Male	20 (62.5%)	22 (57.9%)		7 (43.8%)	14 (73.7%)	
Female	12 (37.5%)	16 (42.1%)		9 (56.3%)	5 (26.3%)	
KPS, median (range)	80 (40–100)	80 (60–100)	*0.035*	79 (60–80)	80 (60–100)	*0.001*
Treatment, no. (%)			0.081			*0.020*
Untreated	4 (12.5%)	1 (2.6%)		4 (25.0%)	0 (0%)	
Single	12 (37.5%)	9 (23.7%)		5 (31.3%)	3 (15.8%)	
Combined	16 (50%)	28 (73.7%)		7 (43.8%)	16 (84.2%)	
IDH, no. (%)			*0.001*			0.489
Mutant	0 (0%)	7 (18.4%)		0 (0%)	2 (10.5%)	
Wild	32 (100%)	31 (81.6%)		16 (100%)	17 (89.5%)	
Involved lobe, no. (%)						
Frontal	4 (12.5%)	12 (31.6%)	0.086	4 (25%)	5 (26.3%)	0.929
Temporal	17 (53.1%)	15 (39.5%)	0.253	5 (31.3%)	8 (42.1%)	0.508
Parietal	6 (18.8%)	6 (15.8%)	0.743	2 (12.5%)	5 (26.3%)	0.415
Occipital	1 (3.1%)	2 (5.3%)	0.660	4 (25%)	1 (5.3%)	0.156
Insular	2 (6.3%)	3 (7.9%)	0.790	1 (6.2%)	0 (0%)	0.457
Callosum	2 (6.3%)	0 (0%)	0.205	0 (0%)	0 (0%)	NA
Hemisphere, no. (%)			0.790			0.312
Unilateral	30 (93.8%)	35 (92.1%)		13 (81.3%)	18 (94.7%)	
Bilateral	2 (6.3%)	3 (7.9%)		3 (18.7%)	1 (5.3%)	
Radiomics signature, median (interquartile range)	−0.284 (−0.687, −0.017)	0.639 (0.238, 0.763)	*< 0.001*	−0.129 (−0.486, 0.175)	0.615 (0.330, 0.824)	*< 0.001*

p values < 0.05 are shown in italics

NA not available

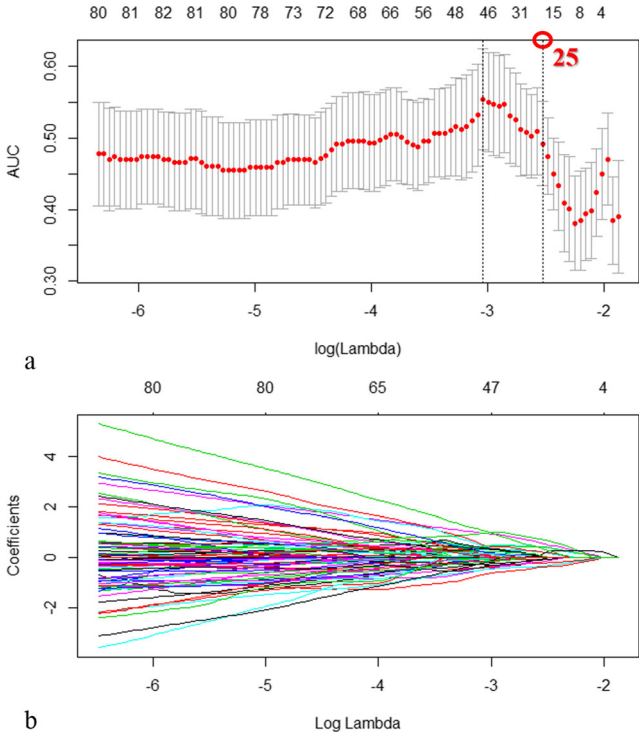

Fig. 2 Radiomics feature selection using the least absolute shrinkage and selection operator (LASSO) algorithm. **a** Selection of the regulation weight λ (Lambda). The AUCs from the LASSO regression cross-validation procedure were plotted as a function of log(λ). The vertical black imaginary lines define the optimal values of λ at which the model provides its best fit to the data. **b** The LASSO coefficient profiles of the 4000 features. The imaginary vertical line was plotted at the selected log(λ) in (**a**), and 25 features with non-zero coefficients were finally identified

factors of sequence and heterogenous region, the sum of absolute coefficients of features extracted from rCET of T1, rEA of T2, and rNEC of FLAIR were 0.880, 0.769, and 0.766, respectively. In addition, the sum of absolute coefficients for each feature type were 1.984 for GLCM feature, 1.812 for histogram statistics, 0.506 for GLRLM feature, and 0.500 for GLSZM feature, respectively.

The evaluation of the radiomics signature and/or clinical risk factors

For the results listed in Table 3, the radiomics signature, age, KPS, and treatment strategy were identified as independent predictors of OS stratification in GBM patients. The multivariable logistic regression model was applied based on three clinical predictors and/or the radiomics signature. The C-index when only three clinical predictors were used for OS stratification was 0.747 (95% CI, 0.719–0.775), and the Hosmer-Lemeshow test produced a value of $p = 0.504$. The C-index that resulted from the use of only the radiomics signature for OS stratification was 0.941 (95% CI, 0.929–0.953), and the Hosmer-Lemeshow test yielded a value of $p = 0.437$. Next, the radiomics signature and clinical predictors were combined to verify the increment in stratification value. The C-index that resulted from the combined use of the radiomics signature and three clinical predictors for OS stratification was 0.971 (95% CI, 0.964–0.980), and the Hosmer-Lemeshow test resulted in a value of $p = 0.921$.

Radiomics nomogram construction and validation

Based on the multivariate logistic regression, a radiomics nomogram that incorporated the radiomics signature and three clinical factors was constructed (Fig. 4). Figure 5a illustrates the calibration curve of the proposed nomogram based on the training cohort. Moreover, a favorable calibration (Fig. 5b) was confirmed in the validation cohort. The C-index was 0.974 (95% CI, 0.961–0.987), and the Hosmer-Lemeshow test produced a value of $p = 0.998$.

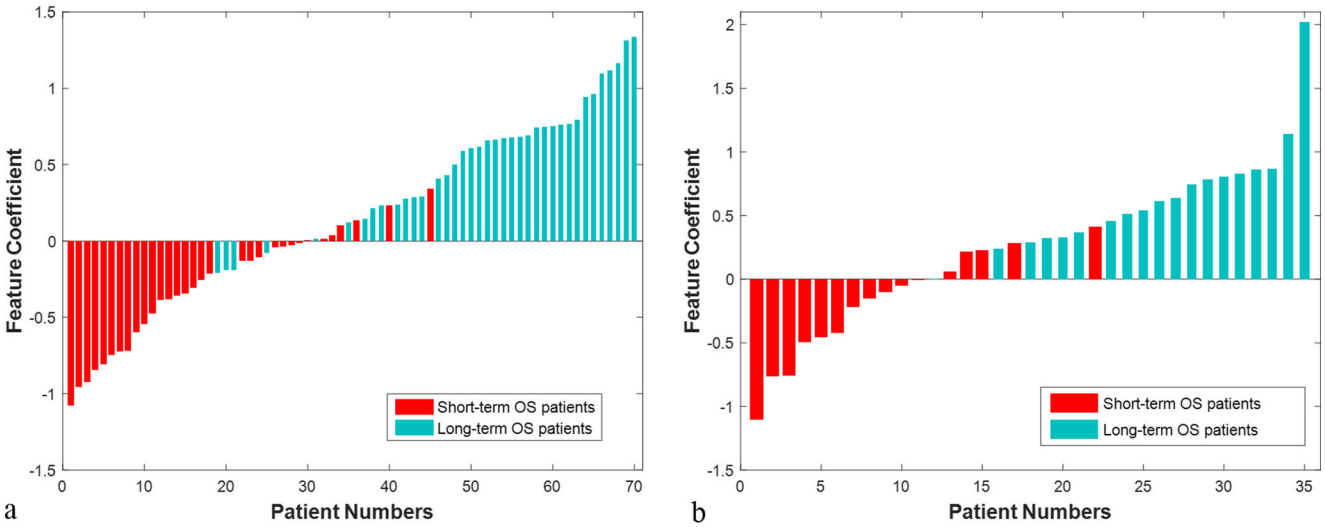

Fig. 3 Radiomics signature for each patient in the (**a**) training cohort and (**b**) validation cohort. The red bars show the radiomics signature values for the patients with short-term overall survival (OS), and the blue bars show the values for those with long-term OS

Table 2 The sums of the absolute values of the feature coefficients from different heterogeneous regions of four MRI sequences

	T1C	T1	T2	FLAIR	Total
rEA	0	0.515	0.766	0.316	1.597
rCET	0	0.880	0.323	0	1.204
rNec	0.040	0	0.322	0.769	1.132
rE/nCET	0.025	0.209	0	0.546	0.779
Total	0.065	1.604	1.412	1.631	4.712

Clinical utility of the radiomics nomogram

The decision curve for the radiomics nomogram (Fig. 6) indicates that the use of the radiomics nomogram to stratify the OS of GBM patients was beneficial at all threshold probabilities in our study.

Discussion

This study investigated the role of radiomics nomogram on overall survival stratification of GBM patients. The radiomics signature, which was constructed based on multiregional imaging features from the multiparametric MRI of each GBM patient, performed better than clinical risk factors in the survival stratification of the GBM patients. Furthermore, the radiomics nomogram integrating both radiomics signature and clinical risk factors could precisely predict the individualized probability of survival stratification for each GBM patient.

Survival-related nomograms of GBM patients constructed in previous studies [8, 20, 33, 34] only have applied some clinical risk factors such as age, gender, KPS, O^6-methylguanine-DNA methyltransferase (MGMT), and IDH status. These clinical factor-based nomograms have got some achievements in survival analysis. In our study, we did not include MGMT information due to the lack of these information on a large proportion of the GBM patients from TCGA. According to the univariable logistic regression model, clinical risk factors, i.e., age, KPS, and way of treatment, were significant in stratifying long- and short-term OS and were chosen to construct a clinical factor-based nomogram. Then, the similar stratification performance was obtained from the clinical factor-based nomogram, comparing to previous studies [8, 20, 33, 34].

Then, the incremental value when adding the radiomics signature into the clinical factor-based nomogram was assessed. The results suggested that the radiomics signature was more robust than the traditional clinical risk factors, as many previous studies focusing on radiomics nomogram indicated [22–25]. To develop the radiomics signature, 4000 high throughput radiomics features were firstly extracted from the multiregional imaging features in the multiparametric MRI of each GBM patient [35] . While, 25 potential features out of 4000 were selected using the LASSO method. The radiomics signature was constructed by the weighted sum of these 25 features (the weights were the corresponding non-zero coefficients). Among these features, the FLAIR sequence and rEA region of GBM contributed more than other MRI sequences and regions. This may be due to more heterogeneous information in rEA region and independent effect of FLAIR sequence for GBM survival prognosis [36]. Thus, the non-invasive radiomics signature derived from multiparametric MRI could serve as a potential imaging biomarker to predict survival stratification.

Table 3 Radiomics signature and clinical factors used for overall survival (OS) stratification of glioblastoma patients

	Univariate logistic regression		Multivariable logistic regression	
	OR (95% CI)	*p*	OR (95% CI)	*p*
Age	0.506 (0.285–0.897)	*0.020*	0.732 (0.257–2.087)	0.559
Gender	0.825 (0.315–2.161)	0.685	NA	
KPS	1.798 (1.050–3.081)	*0.033*	3.807 (1.011–14.337)	*0.048*
Treatment	1.768 (1.054–2.965)	*0.031*	3.361 (1.062–10.640)	*0.039*
IDH	4.378 (0.813–23.904)	0.098	NA	
Frontal	3.231 (0.925–11.290)	0.066	NA	
Temporal	0.575 (0.222–1.490)	0.255	NA	
Parietal	0.813 (0.234–2.820)	0.774	NA	
Occipital	1.722 (0.149–19.918)	0.663	NA	
Insular	1.286 (0.201–8.213)	0.791	NA	
Callosum	1.915 (0.744–15.230)	0.832	NA	
Hemisphere	1.286 (0.201–8.213)	0.791	NA	
Radiomics signature	40.273 (6.454–251.298)	*< 0.001*	87.272 (7.453–121.934)	*< 0.001*

p values < 0.05 are shown in italics

NA not available

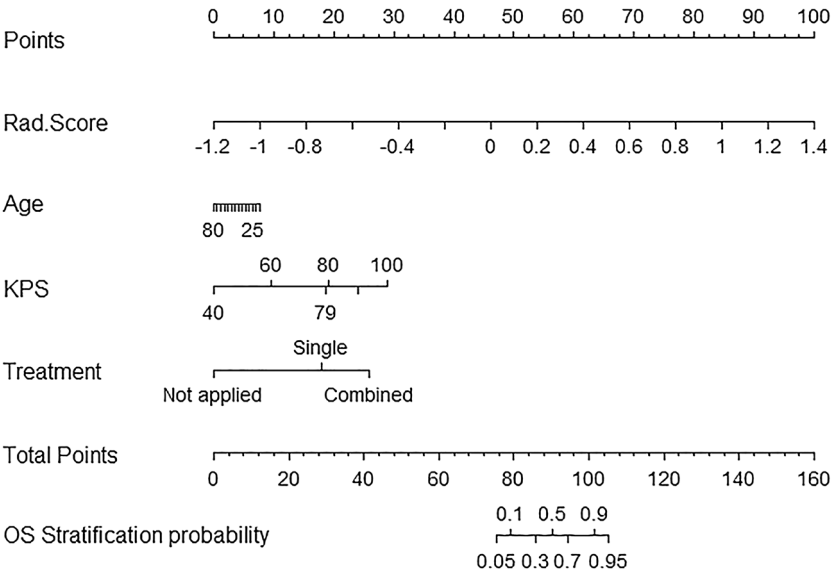

Fig. 4 Radiomics nomogram for the overall survival (OS) stratification of glioblastoma patients

Finally, the combination of the radiomics signature and clinical predictors demonstrated an enhanced stratification efficacy in both the training and validation cohorts. The results indicated that long-term survivors of GBM are more likely to be younger, have a good KPS, undergo neoadjuvant chemoradiotherapy after surgery, and achieve a higher radiomics signature value. Comparing to several survival analysis studies of GBM patients [9, 35, 37], the focus of this study was the proposed radiomics nomogram, which integrated radiomics signature and three clinical predictors, and can visually and individually estimate the probability of survival stratification for each GBM patient. Another important issue associated with this radiomics nomogram is its efficiency in guiding clinical decisions. According to the DCA, when a specific GBM patient is indicated to have a long-term OS by the proposed radiomics nomogram, the adoption of a proper intervention strategy would facilitate the patient outcome. The results suggest that the radiomics nomogram demonstrated great potential for clinical application in the survival stratification of GBM patients.

In our study, the absolute values of coefficients obtained by the LASSO algorithm indicate the contribution of specific feature for OS stratification. For different heterogeneous regions, the features from entire anomaly region (rEA) contributed more to the survival stratification than did the features from other regions, according to their higher sum of absolute coefficients. Most GBM prognosis-related studies indicated the association between poor prognosis and radiomics features from contrast-enhanced region [38, 39]. Some recent studies also revealed the role of features from peritumoral brain parenchyma [5, 37] and from central necrosis [40, 41]. Therefore, it was reasonable that the non-zero-coefficient features from rEA

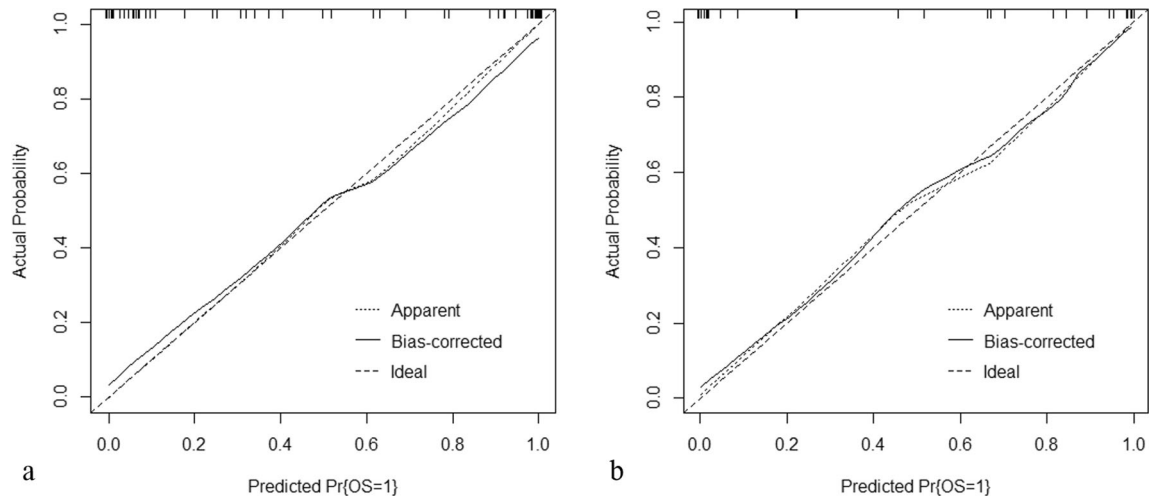

Fig. 5 The calibration curves of the radiomics nomogram in the training cohort (**a**) and validation cohort (**b**). The calibration curves depict the calibration of the nomogram in terms of the agreement between the predicted risk of long-term overall survival (OS) and the observed OS

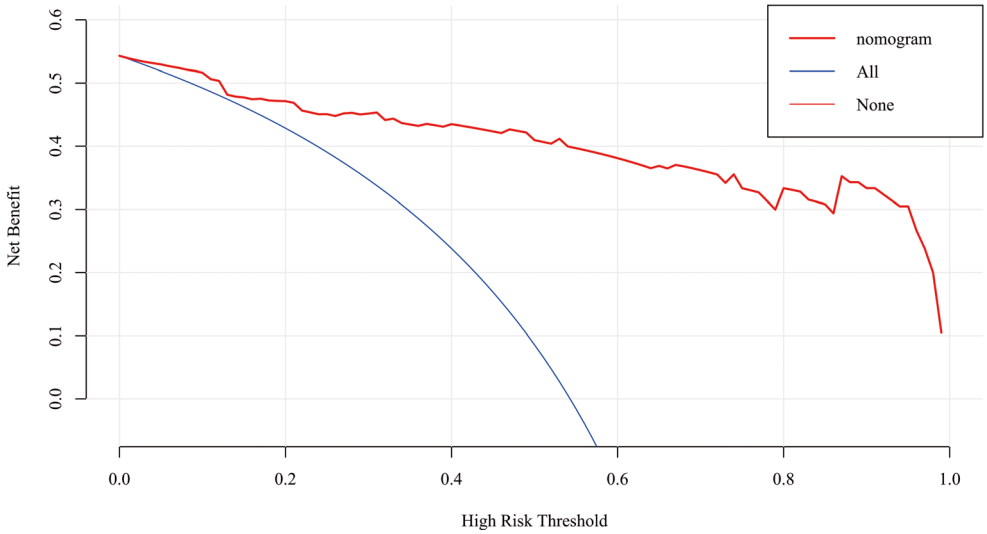

Fig. 6 Decision curve analysis (DCA) for the proposed radiomics nomogram. The *y*-axis represents the net benefit. The *x*-axis represents the threshold probability. The black line at the bottom represents the hypothesis that no patients had long-term overall survival (OS). The blue line represents the hypothesis that all patients had long-term OS. The red line represents the net benefit of the radiomics nomogram at different threshold probabilities

of all the MRI sequences could contain most of the details of heterogenous regions in GBM and could better describe the prognosis of GBM patients than features from each single region. For different MRI sequences, features from the FLAIR images contributed more to the OS stratification model than did features from other sequences, due to their higher sum of absolute coefficients. Especially, both the top 2 and 3 features of all the 25 selected features, i.e., the sum variance (GLCM feature) and kurtosis (top 3 histogram statistics), were from FLAIR image These results were partly consistent with previous studies [5]. These results further suggested the role of information contained in non-contrast-enhanced subregions and sequences for GBM prognosis.

Some limitations of this study were necessary to be further investigated. First, the data used in this study was from TCGA. Although the multiinstitutional data can guarantee the clinical generalizability and usefulness of the radiomics nomogram, a large-scale validation study should be performed prior to its clinical application. Bakas et al [42] collected 135 patients from TCGA, which was more than 105 patients in our study. Because neuroradiologists in our study use the relatively strict exclusion criterion to exclude all the MRI data that appeared to be postoperative in order to avoid bias caused by the visual MRI assessment, the number of enrolled subjects is relatively small. Second, the 2D manual segmentation applied in this study may induce bias about tumor slices selection and manual ROIs delineation. Therefore, a reproducibility analysis was carried out to validate the reproducibility of ROI delineated, describing in Data Supplement S5 of Appendix E1 [43]. Furthermore, Hainc N et al [43] have investigated that the variation of slices and ROI delineation method could affect the radiomics features. These findings could be the guidance in our future work. Finally, although with high efficiency and sparsity, LASSO regression method may be less stable when a large number of features were involved in the model. Other feature selection methods should be investigated in the future work.

In conclusion, this study developed and validated a radiomics nomogram based on multiparametric MRI and multiregional information. Based on the multiinstitutional data from TCGA, the radiomics nomogram demonstrated a favorable predictive accuracy and provided an individualized probability of survival stratification for each GBM patient, which suggests its great potential for clinical application.

Funding This study has received funding by National Nature Science Foundation of China (No. 81701658 to Xi Zhang and No.81801655 to Qiang Tian), Military Science Foundation of China (No. BWS14J038 to Yang Liu), and National Key Research and Development Program of China (No. 2017YFC0107403 to Hongbing Lu).

Compliance with ethical standards

Guarantor The scientific guarantor of this publication is Hongbing Lu.

Conflict of interest The authors of this manuscript declare no relationships with any companies, whose products or services may be related to the subject matter of the article.

Statistics and biometry One of the authors, Xiaopan Xu, has significant statistical expertise.

Informed consent Written informed consent was not required for this study because all the patient data in TCGA was deidentified.

Ethical approval Institutional Review Board approval was not required because all the data used in this study were selected from the Cancer Genome Atlas (TCIA). After ethical review by NIH, the TCIA is freely available for the scientific research. Followed by the instructions of TCIA, we have referred related articles about TCIA.

Study subjects or cohorts overlap Some study subjects or cohorts have been previously reported in AJNR (Am J Neuroradiol. 2017. https://doi.org/10.3174/ajnr.A5279).

Methodology
• retrospective
• diagnostic or prognostic study
• multicenter study

References

1. Ostrom QT, Gittleman H, Stetson L, Virk SM, Barnholtz-Sloan JS (2015) Epidemiology of gliomas. Cancer Treat Res 163:1–14
2. Van Meir EG, Hadjipanayis CG, Norden AD, Shu HK, Wen PY, Olson JJ (2010) Exciting new advances in neuro-oncology: the avenue to a cure for malignant glioma. CA Cancer J Clin 60:166–193
3. Smoll NR, Schaller K, Gautschi OP (2013) Long-term survival of patients with glioblastoma multiforme (GBM). J Clin Neurosci 20:670–675
4. Sottoriva A, Spiteri I, Piccirillo SG et al (2013) Intratumor heterogeneity in human glioblastoma reflects cancer evolutionary dynamics. Proc Natl Acad Sci U S A 110:4009–4014
5. Prasanna P, Patel J, Partovi S, Madabhushi A, Tiwari P (2017) Radiomic features from the peritumoral brain parenchyma on treatment-naive multi-parametric MR imaging predict long versus short-term survival in glioblastoma multiforme: preliminary findings. Eur Radiol 27:4188–4197
6. Zhou M, Scott J, Chaudhury B et al (2018) Radiomics in brain tumor: image assessment, quantitative feature descriptors, and machine-learning approaches. AJNR Am J Neuroradiol 39:208–216
7. Laws ER, Parney IF, Huang W et al (2003) Survival following surgery and prognostic factors for recently diagnosed malignant glioma: data from the glioma outcomes project. J Neurosurg 99:467–473
8. Gately L, McLachlan SA, Philip J, Ruben J, Dowling A (2018) Long-term survivors of glioblastoma: a closer look. J Neurooncol 136:155–162
9. Kickingereder P, Burth S, Wick A et al (2016) Radiomic profiling of glioblastoma: identifying an imaging predictor of patient survival with improved performance over established clinical and radiologic risk models. Radiology 280:880–889
10. Bedard PL, Hansen AR, Ratain MJ, Siu LL (2013) Tumour heterogeneity in the clinic. Nature 501:355–364
11. Fouke SJ, Benzinger T, Gibson D, Ryken TC, Kalkanis SN, Olson JJ (2015) The role of imaging in the management of adults with diffuse low grade glioma: a systematic review and evidence-based clinical practice guideline. J Neurooncol 125:457–479
12. Aerts HJ (2016) The potential of radiomic-based phenotyping in precision medicine: a review. JAMA Oncol 2:1636–1642
13. Gutman DA, Cooper LA, Hwang SN et al (2013) MR imaging predictors of molecular profile and survival: multi-institutional study of the TCGA glioblastoma data set. Radiology 267:560–569
14. Jain R, Poisson LM, Gutman D et al (2014) Outcome prediction in patients with glioblastoma by using imaging, clinical, and genomic biomarkers: focus on the nonenhancing component of the tumor. Radiology 272:484–493
15. Itakura H, Achrol AS, Mitchell LA et al (2015) Magnetic resonance image features identify glioblastoma phenotypic subtypes with distinct molecular pathway activities. Sci Transl Med 7:303ra138
16. Shukla G, Alexander GS, Bakas S et al (2017) Advanced magnetic resonance imaging in glioblastoma: a review. Chin Clin Oncol 6:40
17. Wu CX, Lin GS, Lin ZX et al (2015) Peritumoral edema on magnetic resonance imaging predicts a poor clinical outcome in malignant glioma. Oncol Lett 10:2769–2776
18. Limkin EJ, Sun R, Dercle L et al (2017) Promises and challenges for the implementation of computational medical imaging (radiomics) in oncology. Ann Oncol 28:1191–1206
19. Lambin P, Leijenaar RTH, Deist TM et al (2017) Radiomics: the bridge between medical imaging and personalized medicine. Nat Rev Clin Oncol 14:749–762
20. Gittleman H, Lim D, Kattan MW et al (2017) An independently validated nomogram for individualized estimation of survival among patients with newly diagnosed glioblastoma: NRG Oncology RTOG 0525 and 0825. Neuro Oncol 19:669–677
21. Gold JS, Gönen M, Gutiérrez A et al (2009) Development and validation of a prognostic nomogram for recurrence-free survival after complete surgical resection of localised primary gastrointestinal stromal tumour: a retrospective analysis. Lancet Oncol 10:1045–1052
22. Lao J, Chen Y, Li ZC et al (2017) A deep learning-based radiomics model for prediction of survival in glioblastoma multiforme. Sci Rep 7:10353
23. Huang YQ, Liang CH, He L et al (2016) Development and validation of a radiomics nomogram for preoperative prediction of lymph node metastasis in colorectal cancer. J Clin Oncol 34:2157–2164
24. Zhang B, Tian J, Dong D et al (2017) Radiomics features of multiparametric MRI as novel prognostic factors in advanced nasopharyngeal carcinoma. Clin Cancer Res 23:4259–4269
25. Wu S, Zheng J, Li Y et al (2017) A radiomics nomogram for the preoperative prediction of lymph node metastasis in bladder cancer. Clin Cancer Res 23:6904–6911
26. The Cancer Genome Atlas Data Portal, <https://tcga-data.nci.nih.gov/docs/publications/tcga/>. Accessed 08 Feb 2019
27. Clark K, Vendt B, Smith K et al (2013) The cancer imaging archive (TCIA): maintaining and operating a public information repository. J Digit Imaging 26:1045–1057
28. Collewet G, Strzelecki M, Mariette F (2004) Influence of MRI acquisition protocols and image intensity normalization methods on texture classification. Magn Reson Imaging 22:81–91
29. Tibshirani R (2011) Regression shrinkage and selection via the Lasso. J R Stat Soc Series B Stat Methodol 73:273–282
30. Iasonos A, Schrag D, Raj GV, Panageas KS (2008) How to build and interpret a nomogram for cancer prognosis. J Clin Oncol 26:1364–1370
31. Balachandran VP, Gönen M, Smith JJ, DeMatteo RP (2015) Nomograms in oncology: more than meets the eye. Lancet Oncol 16:e173–e180
32. Vickers AJ, Elkin EB (2006) Decision curve analysis: a novel method for evaluating prediction models. Med Decis Making 26:565–574
33. Cheng W, Zhang C, Ren X et al (2017) Treatment strategy and IDH status improve nomogram validity in newly diagnosed GBM patients. Neuro Oncol 19:736–738
34. Gorlia T, van den Bent MJ, Hegi ME et al (2008) Nomograms for predicting survival of patients with newly diagnosed glioblastoma: prognostic factor analysis of EORTC and NCIC trial 26981-22981/CE.3. Lancet Oncol 9:29–38
35. Chaddad A, Sabri S, Niazi T, Abdulkarim B (2018) Prediction of survival with multi-scale radiomic analysis in glioblastoma patients. Med Biol Eng Comput 56:2287–2300
36. Boxerman JL, Zhang Z, Safriel Y et al (2018) Prognostic value of contrast enhancement and FLAIR for survival in newly diagnosed glioblastoma treated with and without bevacizumab: results from ACRIN 6686. Neuro Oncol 20:1400–1410
37. Wang K, Wang Y, Fan X et al (2016) Radiological features combined with IDH1 status for predicting the survival outcome of glioblastoma patients. Neuro Oncol 18:589–597

38. Brynolfsson P, Nilsson D, Henriksson R et al (2014) ADC texture–an imaging biomarker for high-grade glioma? Med Phys 41:101903
39. Chaddad A, Tanougast C (2016) Extracted magnetic resonance texture features discriminate between phenotypes and are associated with overall survival in glioblastoma multiforme patients. Med Biol Eng Comput 54:1707–1718
40. Liu S, Wang Y, Xu K et al (2017) Relationship between necrotic patterns in glioblastoma and patient survival: fractal dimension and lacunarity analyses using magnetic resonance imaging. Sci Rep 7:8302
41. Ellingson BM, Harris RJ, Woodworth DC et al (2017) Baseline pretreatment contrast enhancing tumor volume including central necrosis is a prognostic factor in recurrent glioblastoma: evidence from single and multicenter trials. Neuro Oncol 19:89–98
42. Bakas S, Akbari H, Sotiras A et al (2017) Advancing the cancer genome atlas glioma MRI collections with expert segmentation labels and radiomic features. Sci Data 4:170117
43. Hainc N, Stippich C, Stieltjes B, Leu S, Bink A (2017) Experimental texture analysis in glioblastoma: a methodological study. Invest Radiol 52:367–373